Supporting Information

Picomolar Fingerprinting of Nucleic Acid Nanoparticles Using Solid-State Nanopores

Mohammad Amin Alibakhshi,[†] Justin R. Halman,[§] James Wilson,[‡] Aleksei Aksimentiev,[‡] Kirill A. Afonin,[§⊥] Meni Wanunu[†#]

[†]Department of Physics and [#]Department of Chemistry and Chemical Biology, Northeastern University, Boston, Massachusetts 02115, United States

[§]Nanoscale Science Program, Department of Chemistry and [⊥]The Center for Biomedical Engineering and Science, University of North Carolina at Charlotte, Charlotte, NC 28223, United States

[‡]Department of Physics, University of Illinois at Urbana–Champaign, 1110 West Green Street, Urbana, Illinois 61801, United States

Sections

I. Compositions of nanoparticles used in this project

RNA ring 5'→3'

nrA:
GGGAACCGUCCACUGGUUCCCGCUACGAGAGCCUGCCUCGUAGC
nrB:
GGGAACCGCAGGCUGGUUCCCGCUACGAGAGAACGCCUCGUAGC
nrC:
GGGAACCGCGUUCUGGUUCCCGCUACGAGACGUCUCCUCGUAGC
nrD:
GGGAACCGAGACGUGGUUCCCGCUACGAGUCGUGGUCUCGUAGC
nrE:
GGGAACCACCACGAGGUUCCCGCUACGAGAACCAUCCUCGUAGC
nrF:
GGGAACCGAUGGUUGGUUCCCGCUACGAGAGUGGACCUCGUAGC

DNA cube with three Ts at each corner 5'→3'

dA:
GGCAACTTTGATCCCTCGGTTTAGCGCCGGCCTTTTCTCCCACACTTTCACG
dB:
GGGAAATTTCGTGGTAGGTTTTGTTGCCCGTGTTTCTACGATTACTTTGGTC
dC:
GGACATTTTCGAGACAGCATTTTTTCCCGACCTTTGCGGATTGTATTTTAGG
dD:
GGCGCTTTTGACCTTCTGCTTTATGTCCCCTATTTCTTAATGACTTTTGGCC
dE:
GGGAGATTTAGTCATTAAGTTTTACAATCCGCTTTGTAATCGTAGTTTGTGT
dF:
GGGATCTTTACCTACCACGTTTTGCTGTCTCGTTTGCAGAAGGTCTTTCCGA

II. Supplementary experimental results

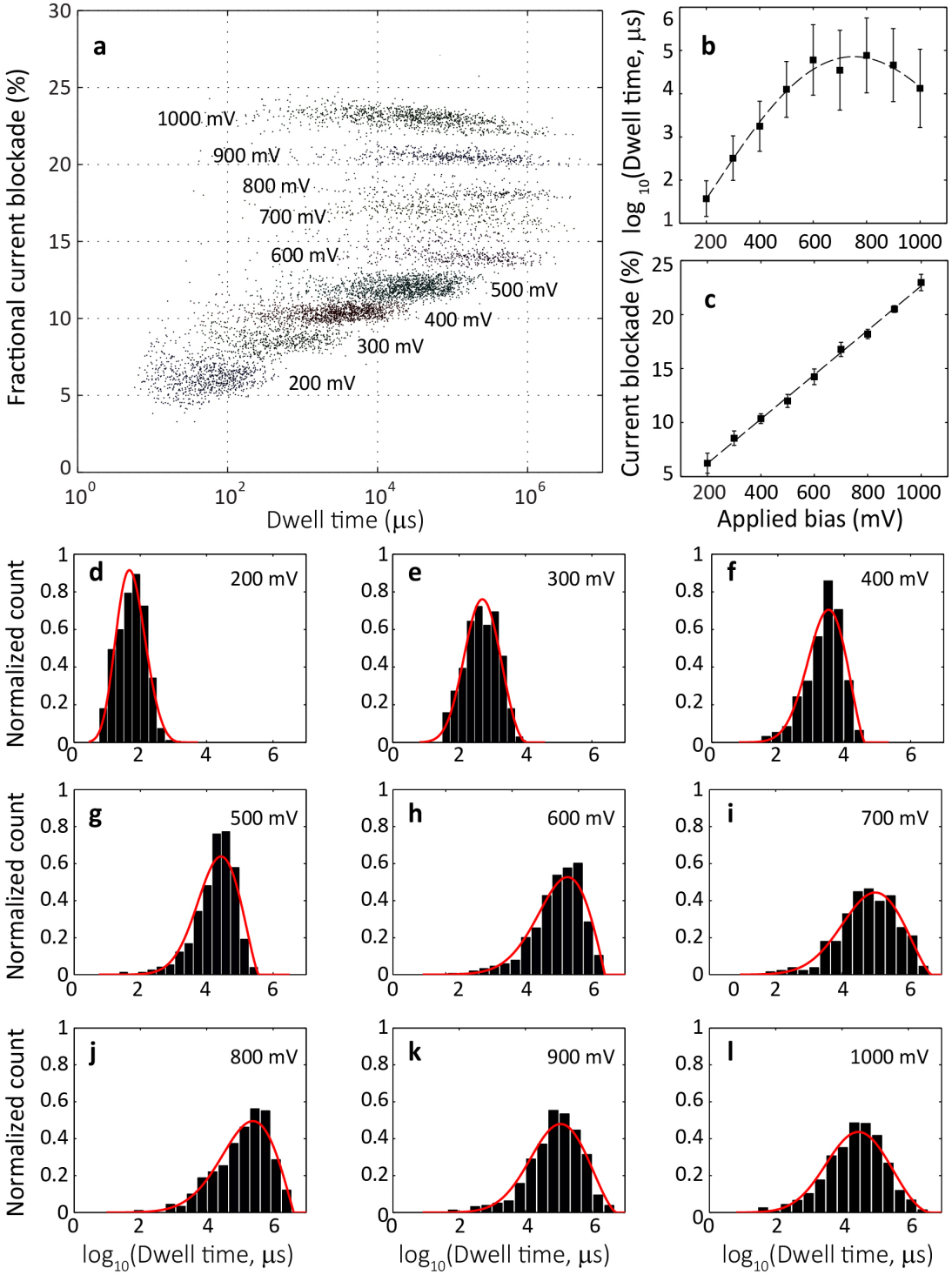

Figure S1. (a) Scatter plot of fractional current blockade and dwell time for translocation of the RNA rings through a 9 nm-diameter nanopore at different voltages. (b) Dwell time versus applied voltage. (c) Fractional current blockade versus applied voltage. (d-l) Dwell time distribution at different applied voltages fitted with the generalized extreme value distributions (red lines). Experiments performed with 400 mM KCl (10 mM Tris, 2mM $MgCl_2$, pH 7.9).

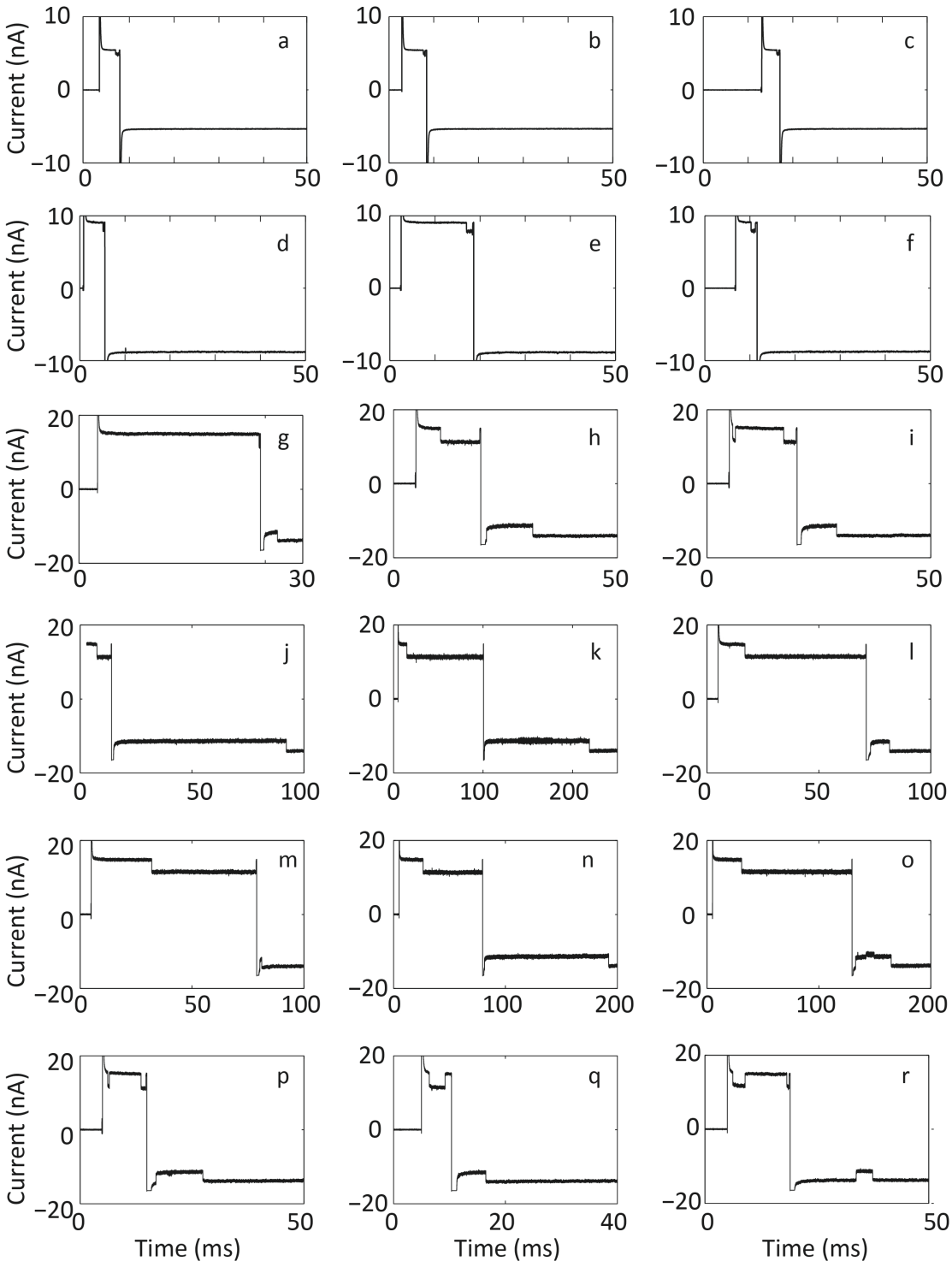

Figure S2. RNA rings after capture at 300 mV (a-c) and 500 mV (d-f) cannot be recaptured after reversing the bias polarity, indicating that current blockade is only due to collision of the rings with the nanopore without translocation. (g-r) Capture and translocation of RNA rings at 900 mV and their recapture at -900 mV. Experiments performed with 400 mM KCl (10 mM Tris, 2mM $MgCl_2$, pH 7.9).

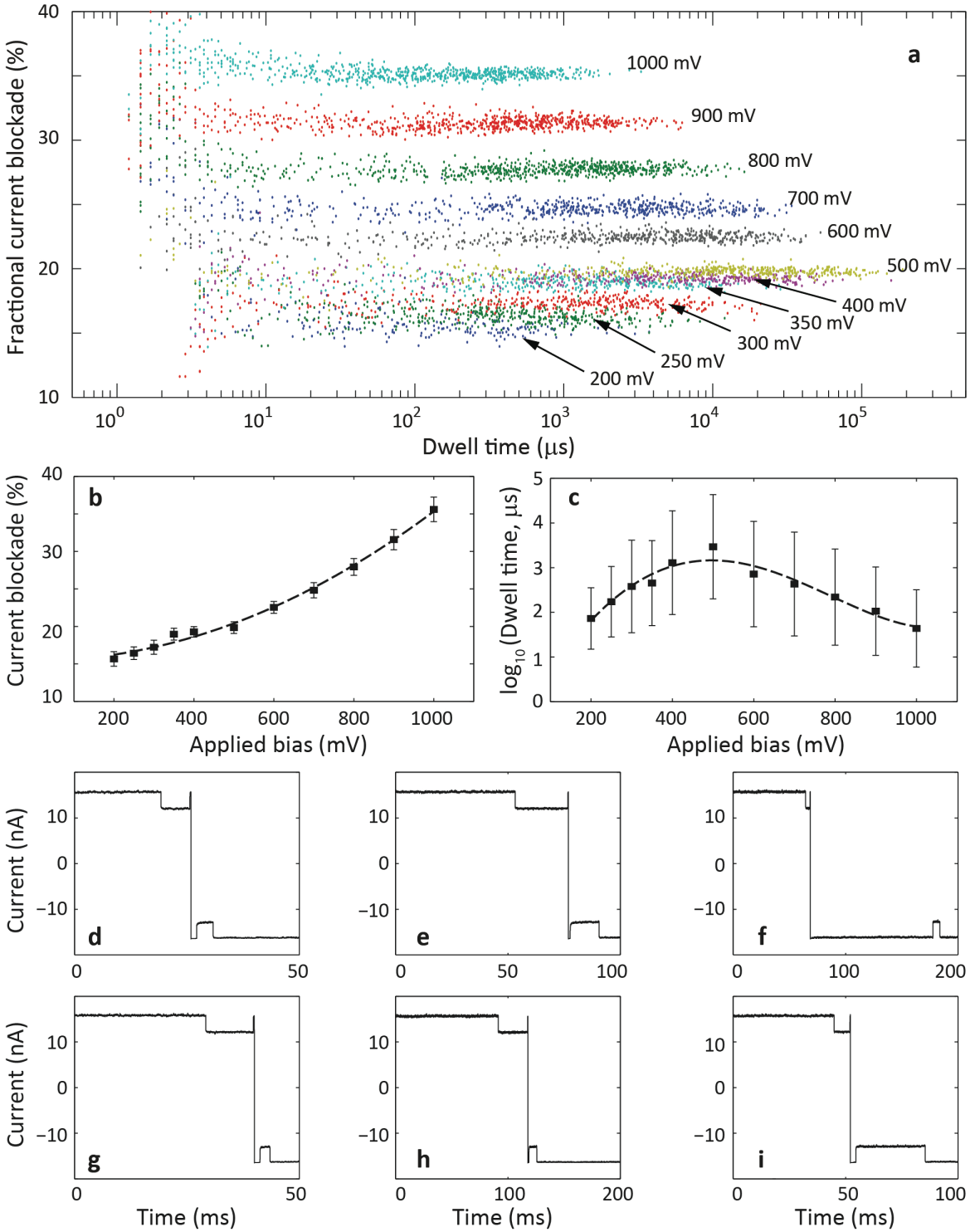

Figure S3. (a) Scatter plot of fractional current blockade and dwell time for translocation of the DNA cubes at different voltages. (b) Fractional current blockade versus applied voltage. (c) Dwell time *versus* applied voltage. (d-i) Recapture of DNA cubes after translocation at 800 mV. Experiments performed with 400 mM KCl (10 mM Tris, 2mM $MgCl_2$, pH 7.9).

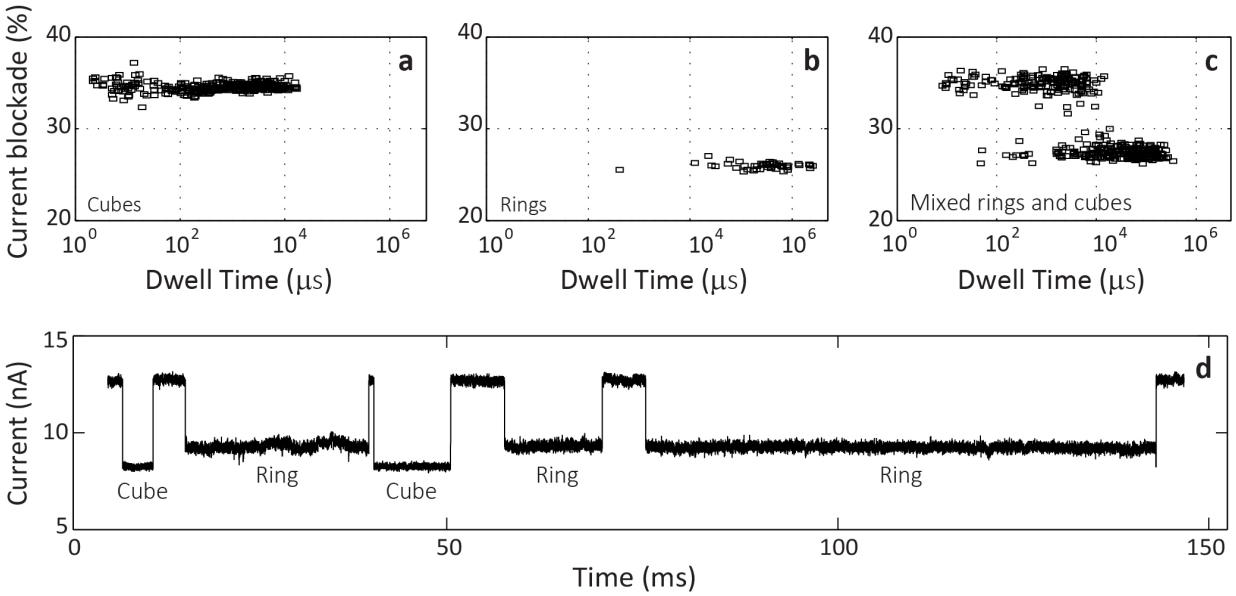

Figure S4. Scatter plot of fractional current blockade and dwell time for translocation of (a) DNA cubes, (b) RNA rings, and (c) mixture of DNA cubes and RNA rings in a 9 nm-diameter nanopore at 1V. (d) Example of a current trace fragment recorded from a cube-ring mixture, the same system as in panel c. Experiments performed with 400 mM KCl (10 mM Tris, 2mM $MgCl_2$, pH 7.9).

III. Estimation of the fractional current blockade

In working with the TEM-drilled nanopores usually an equivalent cylindrical pore with an effective pore length equal to one-third of the membrane thickness is used.[1] The fractional current blockade when a spherical analyte traverses a cylindrical pore can be calculated as

$$i = 1 - \frac{R_0}{R_b} \tag{S1}$$

wherein R_0 is the open pore resistance, $R_0 = \frac{1}{\sigma D} + 4L/\sigma\pi D^2$, and R_b is the resistance of the pore partially blocked by the analyte:

$$R_b = \frac{1}{\sigma D} + \frac{1}{\sigma}\int_0^L \frac{dx}{A(x)} = \frac{1}{\sigma D} + 4\frac{L-d}{\sigma\pi D^2} + 4\,\frac{atan\left(\frac{d}{\sqrt{D^2-d^2}}\right)}{\sigma\pi\sqrt{D^2-d^2}} \tag{S2}$$

L and D are the pore length and diameter, d is the analyte diameter, σ is the salt conductivity, and the equation is derived for the case of $L > d$. Moreover, the $\frac{1}{\sigma D}$ term accounts for the access resistance of the pore. This equation is plotted in Figure S5b for a 9 nm-diameter nanopore with different lengths. It can be seen that when the analyte diameter to nanopore diameter ratio (d/D) is 0.5, only ~4% fractional blockade is obtained. This value reaches 20% when the size ratio increases to 0.8 (for $L = 20$ nm). For the DNA cubes with a globular structure and the radius of gyration of ~4.4 nm ($d =$ 8.8 nm) obtained from the MD simulations (Figure S5a), equation S2 yields 43% blockade ($D = 9.5$ nm, $L = 20$ nm) which is consistent with the experimental results presented in Figures 4d, i.e., 35% blockade at 800 mV. Use of the radius of gyration for the RNA rings to estimate the fractional blockade is not justified, as the RNA rings have a planar structure. It's worthy of attention that although this calculation provides a rough estimate of the fractional blockade of the cubes in the nanopores, it cannot explain the monotonic increase of the fractional blockade with the applied bias. In fact this equation is based on the assumptions of a fixed shape for the analyte and uniform distribution of the electric field in the nanopore, which is not accurate for the TEM-drilled hourglass-shaped nanopores.

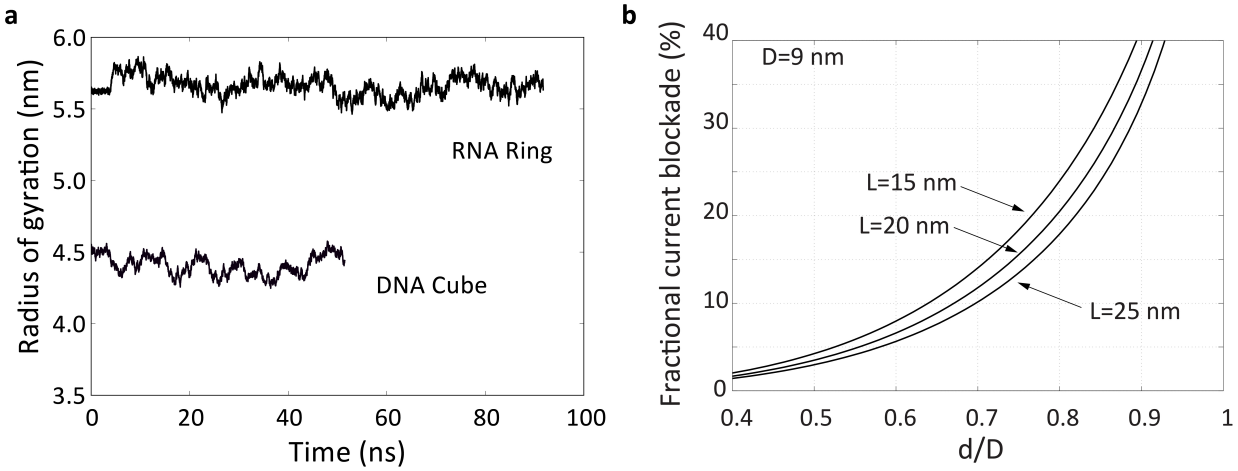

Figure S5. (a) Fractional blockade of a *D*=9 nm cylindrical pore with different lengths. (b) Radius of gyration of the DNA cubes and the RNA rings obtained from MD simulations.

IV. Molecular dynamics simulations of translocation of NANPs through a nanopore

Table S1: Summary of simulations performed. Two NANPs were simulated: the DNA cube and the RNA ring, as well as an empty pore. The cubes were simulated starting from three orientations differing by the part of the cube that was closest to the nanopore constriction (see SI Figure S5). The blockade current was measured after the particles reached a stable position within the nanopore; the time elapsed from the beginning of the simulation before each particle reached such stable position is specified in the table as t_S.

NA Particle	Voltage	Simulation time	Orientation	t_S (ns)	Current (nA)
Cube	200 mV	98 ns	Flat	20 ns	5.32±0.08
Cube	200 mV	97 ns	Corner	20 ns	5.71±0.06
Cube	200 mV	99 ns	Edge	35 ns	5.85±0.07
Cube	500 mV	70 ns	Flat	25 ns	13.53±0.11
Cube	500 mV	70 ns	Edge	25 ns	14.94±0.09
Cube	500 mV	70 ns	Corner	N/A	N/A
Ring	200 mV	116 ns	Vertical	60 ns	7.04±0.07
Ring	200 mV	88 ns	Vertical	20 ns	6.34±0.08
Ring	500 mV	109 ns	Vertical	25 ns	16.43±0.08
Ring	500 mV	84 ns	Vertical	12 ns	16.61±0.09
Empty	200 mV	57 ns	N/A	20 ns	7.14±0.10
Empty	500 mV	48 ns	N/A	10 ns	17.33±0.11

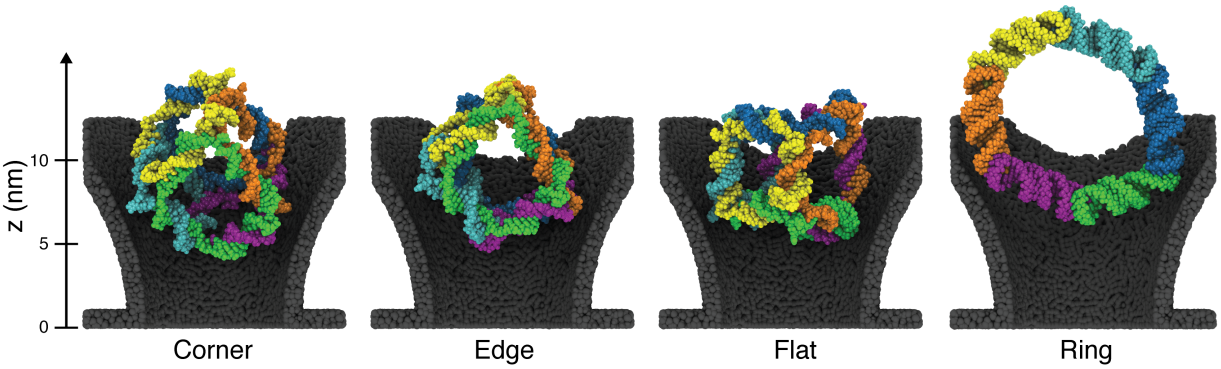

Figure S6. Initial orientation of the NANPs in MD simulations of nanopore transport. The nanopore surface is shown in gray, separate strands of the NA nanoparticles are shown in different colors.

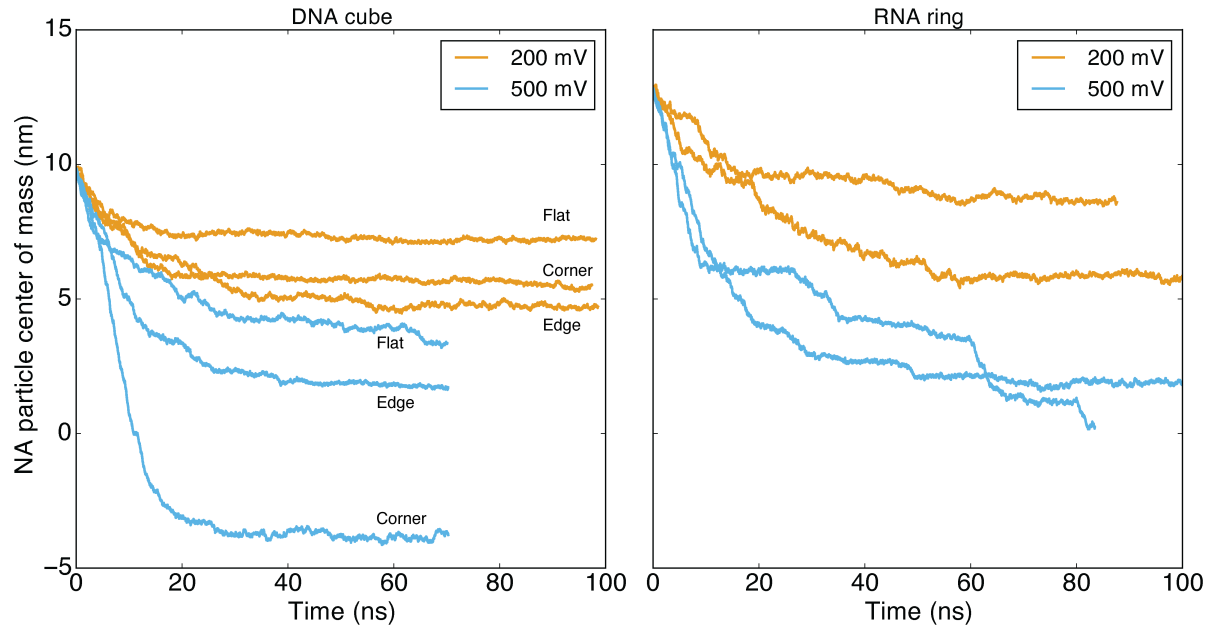

Figure S7. Simulated displacement of NANPs through a solid-state nanopore. Z-coordinate of the particle's center of mass is plotted *versus* simulation time. The z-coordinate is aligned with the pore axis and attains zero at the trans end of the nanopore. Data shown in the left and right panels correspond to the simulations of the DNA cubes and RNA rings, respectively. In both panels, orange and blue lines indicate the outcomes of the simulations performed under 200 and 500 mV bias, respectively.

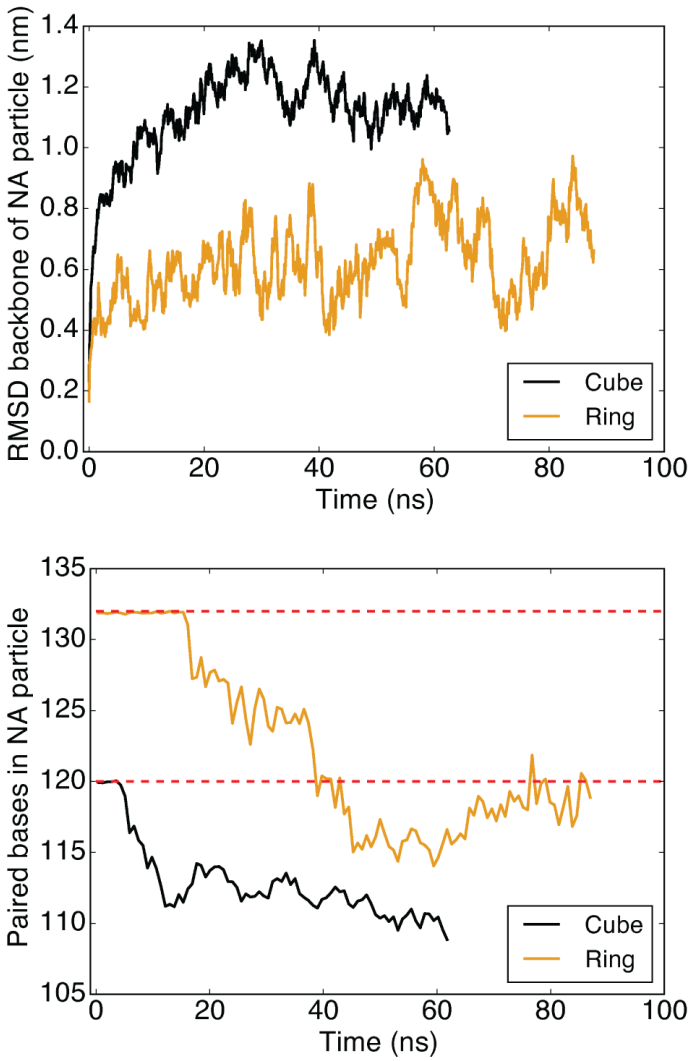

Figure S8. Structural fluctuations of NANPs in bulk solution. (Top) RMSD of the NANPs from their idealized initial conformation during the few equilibration simulations. The RMSD was computed using coordinates of the NA backbone atoms. (Bottom) Number of bases paired in the NANPs during the free equilibration simulations. Red dashed lines indicate the number of basepairs measured for the idealized geometry of the particles.

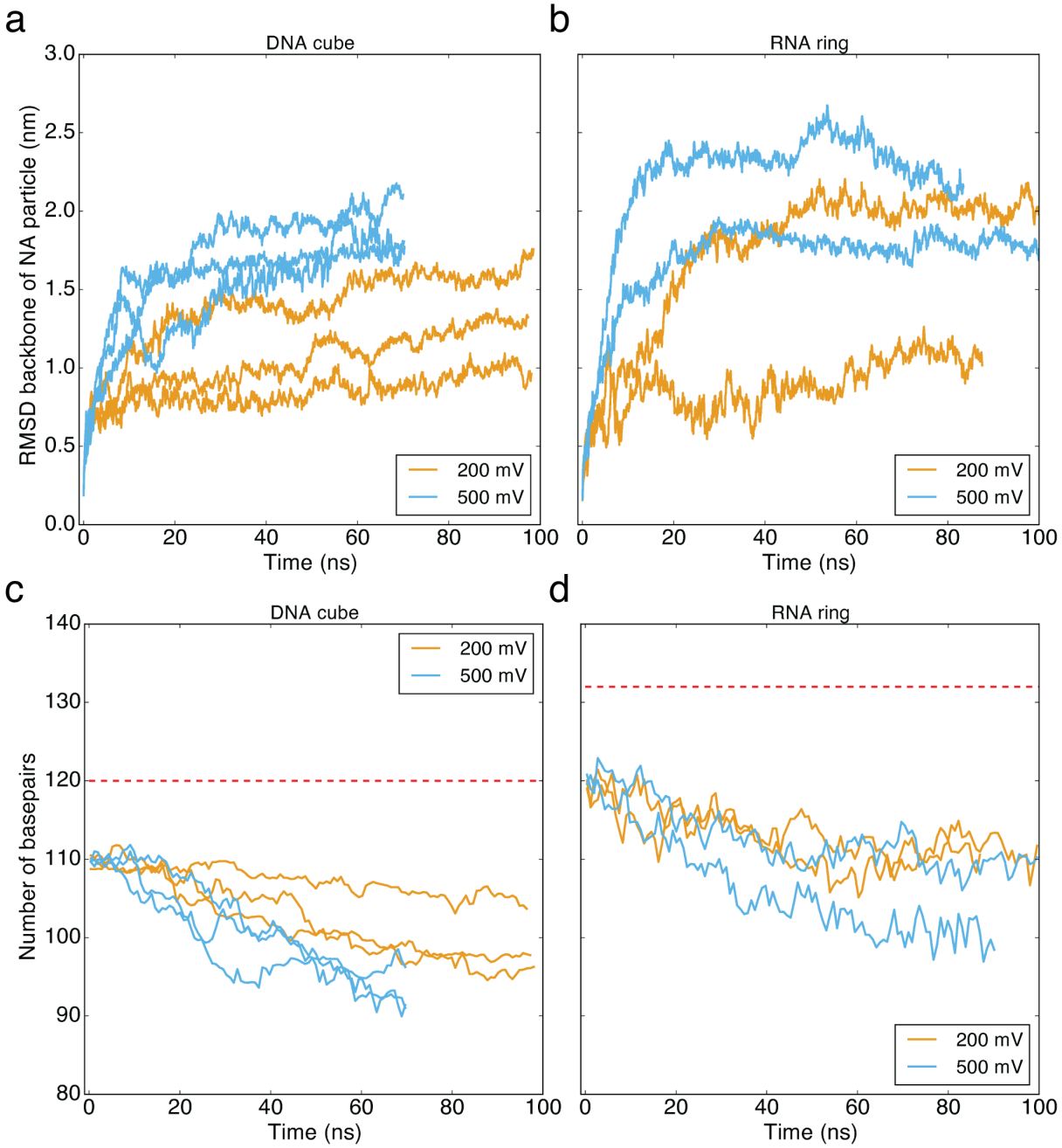

Figure S9. Structural integrity of NANPs during simulated nanopore translocation. (a,b) RMSD of the NANPs from their idealized initial conformations during the nanopore transport simulations. The RMSD was computed using coordinates of the NA backbone atoms. Data in panels a and b derived from the simulations of the DNA cubes and RNA rings, respectively. In both panels, orange and blue lines indicate the outcomes of the simulations performed under 200 and 500 mV bias, respectively. (c,d) Number of intact basepairs in NANPs during the nanopore transport simulations. Red dashed lines indicate the number of basepairs measured for the idealized geometry of the particles.

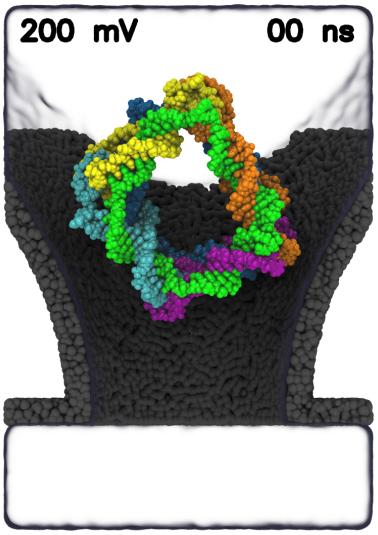

Animation M1. Animation illustrating a 99 ns MD trajectory of a DNA cube translocation through a solid-state nanopore. The simulation began having the edge of the DNA cube pointing toward the nanopore constriction. The simulation was performed under a 200 mV bias.

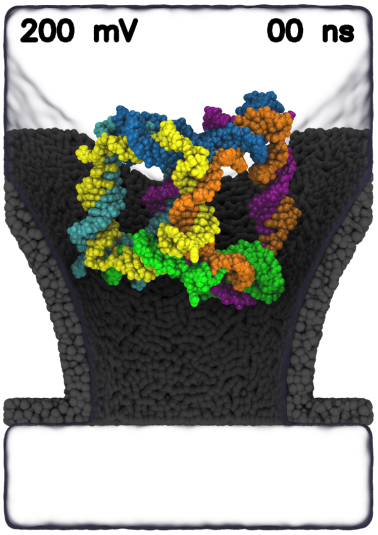

Animation M2. Animation illustrating a 98 ns MD trajectory of a DNA cube translocation through a solid-state nanopore. The simulation began with a face of the DNA cube pointing toward the nanopore constriction. The simulation was performed under a 200 mV bias.

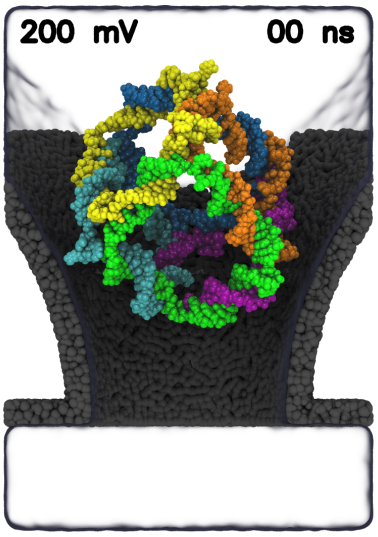

Animation M3. Animation illustrating a 97 ns MD trajectory of a DNA cube translocation through a solid-state nanopore. The simulation began having a corner of the DNA cube pointing toward the nanopore constriction. The simulation was performed under a 200 mV bias.

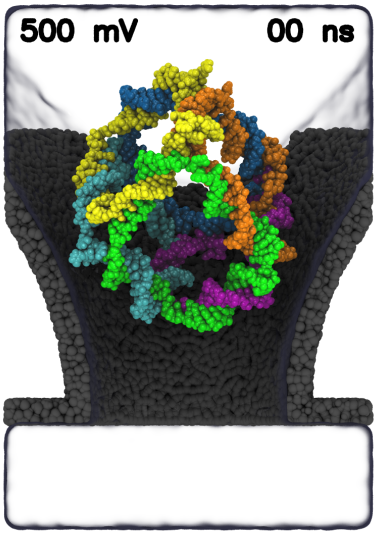

Animation M4. Animation illustrating a 70 ns MD trajectory of a DNA cube translocation through a solid-state nanopore. The simulation began having a corner of the DNA cube pointing toward the nanopore constriction. The simulation was performed under a 500 mV bias.

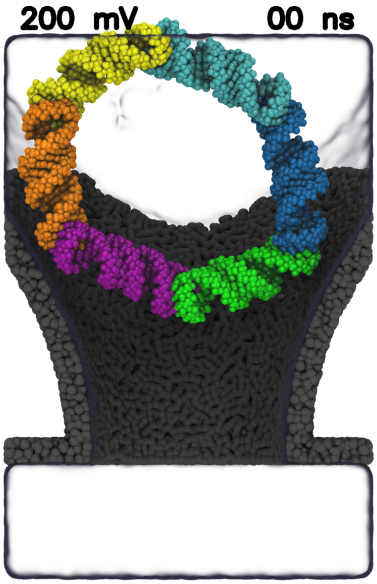

Animation M5. Animation illustrating a 115 ns MD trajectory of an RNA ring translocation through a solid-state nanopore. The simulation began having the ring centered in the nanopore, and the axis of the nanopore in the plane of the ring. The simulation was performed under a 200 mV bias.

REFERENCES

1. Kim, M. J.; Wanunu, M.; Bell, D. C.; Meller, A., Rapid Fabrication of Uniformly Sized Nanopores and Nanopore Arrays for Parallel DNA Analysis. *Adv. Mater.* **2006,** *18*, 3149-3153.